

Proceeding of the Korean Nuclear Society Spring Meeting  
Cheju, Korea, May 2001

## Return Momentum Effect on Reactor Coolant Water Level Distribution during Mid-Loop Conditions

Jae Kwang Seo

Korea Atomic Energy Research Institute  
150 Dukjin-dong, Yusong-gu, Taejon 305-353, Korea

Jae Young Yang

Korea Power Engineering Company  
150 Dukjin-dong, Yusong-gu, Taejon 305-353, Korea

Goon Cherl Park

Department of Nuclear Engineering  
Seoul National University  
San 56-1, Shillim-dong, Kwanak-gu, Seoul 151-742, Korea

### Abstract

An accurate prediction of the Reactor Coolant System (RCS) water level is of importance in the determination of the allowable operating range to ensure safety during mid-loop operations. However, complex hydraulic phenomena induced by the Shutdown Cooling System (SCS) return momentum causes different water levels from those in the loop where the water level indicators are located. This was apparently observed at the pre-core cold hydro test of the Yonggwang Nuclear Unit 3 (YGN 3) in Korea. In this study, in order to analytically understand the effect of the SCS return momentum on the RCS water level distribution, a model using a one-dimensional momentum and energy conservation for cylindrical channel, hydraulic jump in operating cold leg, water level build-up at the Reactor Vessel (RV) inlet nozzle, Bernoulli constant in downcomer region, and total water volume conservation has been developed. The model predicts the RCS water levels at various RCS locations during the mid-loop conditions and the calculation results were compared with the test data. The analysis shows that the hydraulic jump in the operating cold legs, in conjunction with the pressure drop throughout the RCS, is the main cause creating the water level differences at various RCS locations. The prediction results provide good explanations for the test data and show the significant effect of the SCS return momentum on the RCS water levels.

## 1. Introduction

In order to perform refueling and steam generator (SG) maintenance activities simultaneously, SGs should be isolated from the radioactive reactor coolant by the SG nozzle dams. The RCS water level must be lowered below the lowest point of the nozzle dams to install the nozzle dams. In many pressurized water reactors (PWRs), the lowest point of the nozzle dams is lower than the top of the hot leg pipe. Therefore, during the nozzle dam installation the free surface of the reactor coolant remains in between the top and bottom of the hot legs : such an operation is called "Mid-Loop Operation". However, this operation involves certain risks to the plant decay heat removal (DHR) capability and loss of DHR (LODHR) accidents during nonpower operation (especially, during mid-loop operation) and its consequences have been of increasing concern for years.

The most frequent reason for the LODHR accidents during the past twenty years is the air binding of the DHR System or the SCS pumps due to vortex formation near the junction of hot leg and the SCS pump suction line resulting from insufficient RCS water level. In most cases, inappropriate indication of the level instruments followed by over drain of the RCS was the direct cause of the accidents. The LODHR accident in the Diablo Canyon plant on April 10, 1987 (USNRC, 1987), was probably the most serious one in this type, resulted in core uncover, which prompted the issue of the US NRC Generic Letter (GL) 88-17 (Crutchfield, 1988).

The GL required the holders of operating license and construction permits for PWRs to improve plant design to rectify the deficiencies in the areas of prevention of accident initiation, mitigation of accidents before they potentially progress to core damage, and control of radioactive material if a core damage accident should occur. The GL emphasized the importance of providing reliable level instruments by the discussions on the RCS level differences during the mid-loop operation. The GL indicated that the causes of the RCS level differences are the driving force necessary to accomplish the SCS flow and the SCS return water momentum.

Despite the importance of these phenomena to the safety in mid-loop operation, efforts to analyze these phenomena have been circumvented due to the difficulties involved and a lack of experimental data (Newton, 1988). Previous works have been concentrated on developing experimental correlations to determine the critical water level incipient of vortex formation and air entrainment using downscaled experimental facilities (Andreychek et al., 1988; Oh, 1991; Chung et al., 1993). However, their results showed large discrepancies so their applications were not acceptable to some plants with narrow mid-loop operation bands. In addition, because (1) these experiments have been performed in downscaled facilities emulating only the portion of the operating hot leg and SCS suction line and (2) the level in the idle hot leg, where the level indicator is located, is expected to be higher than that in the operating hot leg, their applicability to real plants is quite limited. Therefore, it is important to develop an analytical tool to accurately assess the RCS water level distribution during mid-loop conditions with and without fuel in the reactor core. In order to prove the validity of the tool for the application of a real plant, it would be the best to be verified against the data obtained at the plants under investigation.

The Korea Electric Power Corporation (KEPCO) and the Korea Atomic Energy Research Institute (KAERI) jointly performed the RCS water level measurements at six different RCS locations of YGN 3. The purpose of the test was to assess the operation range in conjunction with the measurements of incipient levels of air entrainment for mid-loop operation. This paper (1) describes the test data of water levels at six legs obtained at YGN 3, and (2) focuses on the analysis of the water level distribution during mid-loop operation with a model developed in this

study.

The objectives of this study are :

(1) to develop a model to predict the RCS water level distribution during mid-loop conditions, (2) to validate the model by comparing the prediction with the test data, (3) to provide the phenomenological understanding of the effect of the SCS return momentum on the water level differences at various RCS locations, and (4) to provide a rudimentary basis for developing future design tools assessing mid-loop operation bands.

Through this effort, the authors intend to identify the important aspects of the RCS water level distribution to be considered in assessing the allowable operating ranges for mid-loop operation.

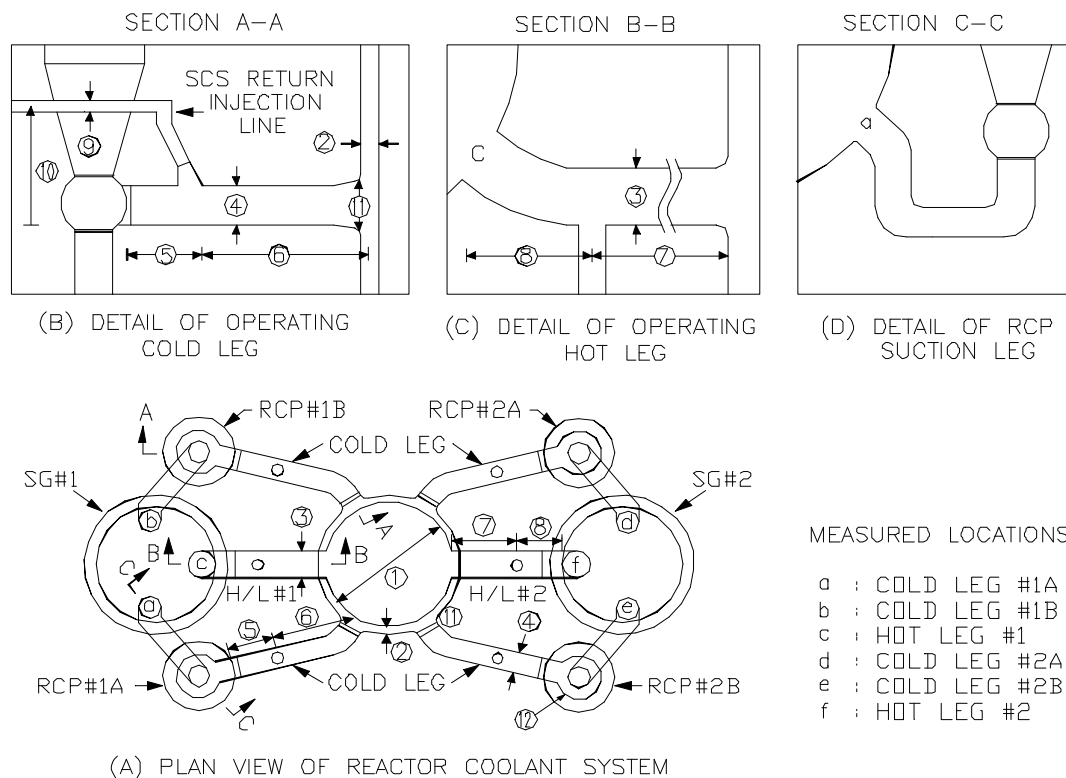


Fig. 1 General view with major components and measured locations

## 2. Description of the test

### 2.1 Description of YGN 3 plant

YGN 3 is a ABB-CE System 80 type PWR plant producing 1000 MWe, consisting of two identical heat transfer loops (see Fig. 1). Each loop is composed of one hot leg and two cold legs. The SCS suction line is connected vertically on the bottom of each hot leg and the SCS return lines (two per loop) are connected to the top of the cold legs with a 60 degree inclination. Table 1 shows the dimensions of components important for the analysis of the test data (the item numbers are correspondingly designated in Fig. 1). The plant was at cold hydro test phase and the reactor core was not installed.

Table 1 Descriptions of YGN 3

Item	Major components related to the analysis	Dimensions
1	Reactor vessel core barrel inside diameter, m	3.556
2	Reactor vessel downcomer gap size, m	0.2286
3	Hot leg inside diameter, m	1.0668
4	Cold leg inside diameter, m	0.762
5	Distance from Reactor Coolant Pump (RCP) casing to the SCS return injection nozzle, m	1.8542
6	Distance from SCS return injection nozzle to downcomer, m	3.9116
7	Distance from SCS suction nozzle to downcomer, m	2.9972
8	Distance from SCS suction nozzle to SG plenum, m	0.5588
9	SCS return injection pipe inside diameter, m	0.254
10	Height of SCS injection pipe relative to cold leg bottom, m	2.6162
11	Void volume of SCS injection pipe, m <sup>3</sup>	0.26
12	RCP casing inside diameter (equivalent diameter considering internal structure), m	0.762

## 2.2 Instrumentation

The level measurements were performed in the inlet and outlet nozzles of the SGs (a - f of Fig. 1) by measuring the distance from the lowest pin hole for the nozzle dam installation to the surface of the water by a ruler. A tygon tube and two differential pressure level transmitters with sensing taps located on each of the SCS suction lines respectively were used to determine the initial reference water levels (initial RWLs). SCS flowrates, SCS pump suction and discharge pressures, and SCS pump currents were also monitored and recorded from the main control room (MCR). SCS pump vibration was measured in the primary auxbuilding and were reported to the MCR by telephone. The RCS water behavior in the operating hot leg was recorded by using a video cassette recorder for later analysis.

## 2.3 Test range

Three initial RWLs for each loop operation were selected. There were four SCS flowrates for each initial RWL, except for initial RWL of - 5.08 cm in the case of loop 2 operation, where the test was not conducted for 17000 LPM (see Table 2).

Table 2 Test conditions

Operating loop	Initial reference water level (relative to hot leg center line, cm )	Flowrate (LPM)				
Loop 1	+ 7.32	9500	11500	13000	15000	17000
	0.0	9500	11500	13000	15000	17000
	- 5.08	9500	11500	13000	15000	17000
Loop 2	+ 5.08	9500	11500	13000	15000	17000
	0.0	9500	11500	13000	15000	17000
	- 5.08	9500	11500	13000	15000	(*)

(\*) The level measurements could not be conducted due to the air entrainment to the SCS pump indicated by both the SCS pump current and vibration monitoring

## 2.4 Test procedure

The RCS water level measurement test (RWLT) was performed in conjunction with the test to measure the incipient level of air entrainment (ILAT). The tests were performed using loop 1 SCS pump first and upon completion of RWLT and ILAT for the loop, both tests were repeated by switching the SCS pump in loop 2. The test procedures were as follows:

- (1) adjust the RCS level to a steady pre-determined initial RWL,
- (2) start SCS pump at the preset lowest flowrate of 9500 LPM,
- (3) wait to reach a steady state and measure/record the test parameters,
- (4) raise the SCS flowrate and repeat (3) for all the flowrates in Table 2,
- (5) repeat (1) through (4) for all the initial RWLs in Table 2.

Caution was given to the operator that the SCS pump current shall be continuously monitored and that if a sudden variation of pump current occurs or an abnormally high pump vibration is reported, the pump shall be stopped immediately to protect the pump from being damaged by air entrainment and record the flowrate as the incipient flowrate of air entrainment for the level and terminate the RWLT.

## 3. Model development

In order to predict the water level and understand the general trend of the level behavior during mid-loop conditions, modeling of hydraulic phenomena expected in the components composing the RCS is required. The review of the RCS pressure drop data indicated that the major source of level difference from the cold leg to the SCS outlet nozzle during mid-loop operation are a 90° flow direction change at the Reactor Vessel (RV) inlet nozzle, flow area change and frictional pressure loss across the complex geometries of flow skirt, flow baffle and lower support structure of the lower RV plenum region and the flow area change at the RV outlet nozzle. To account for these, the basic mass continuity equation, one-dimensional momentum equation, empirical head loss equation, and Bernoulli equation are incorporated in the model. In addition, the hydraulic jump model is introduced to explain the overall water level trends. In first part of this section, equations and parameters with which the level profile of the flow in a horizontal pipe can be determined conveniently are derived and defined. Second part of this section describes the necessary equations and the calculational scheme to link these equations in the sequence of flow path.

### 3.1 General method for not fully filled horizontal pipe flow

For the general flow in a pipe shown in Fig. 2, a one-dimensional momentum equation is written as

$$PA - (P + dP)(A + dA) - t_w P_e dx + rVA - rVA(V + dV) = 0. \quad (1)$$

Mass continuity equation for an incompressible flow is

$$VA = (V + dV)(A + dA). \quad (2)$$

By combining equations (1) and (2) and neglecting the terms of small order, we get:

$$-\frac{dP}{dx} - \frac{t_w P_e}{A} - \frac{(P - rV^2)}{A} \frac{dA}{dx} = 0. \quad (3)$$

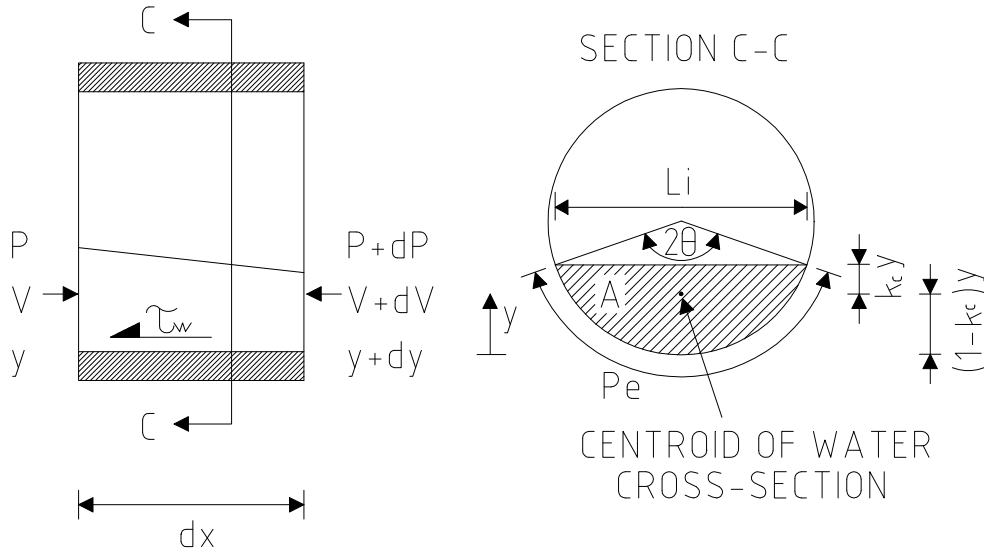


Fig. 2 General flow geometry

The pressure is essentially hydrostatic and defined as the area-averaged pressure for the water cross section as follows:

$$P = k_c r g y, \quad (4)$$

where the centroid parameter of the water cross section is given by the following equation:

$$k_c = \frac{[-q \cos q + \sin q - \frac{\sin^3 q}{3}]}{[(1 - \cos q)(q - \sin q \cos q)]}. \quad (5)$$

The term  $k_c y$  represents the distance from the free surface to the centroid of the water cross section. Upon differentiation of equation (4) with respect to the axial coordinate:

$$\frac{dP}{dx} = r g \frac{d(k_c y)}{dx}. \quad (6)$$

It can be shown that by substituting equations (4) and (6) into equation (3) and using the simplification method shown in the Reference (Sadatomi et al., 1993), equation (3) reduces to

$$\frac{dy}{dx} = \frac{-t_w P_e}{r g A - L_i r V^2} = \frac{-t_w P_e}{r g A} \frac{1}{(1 - Fr^2)}. \quad (7)$$

Froude number,  $Fr$ , and shear stress at the fluid-wall boundary,  $t_w$ , are defined by

$$Fr = \sqrt{\frac{L_i V^2}{g A}}. \quad (8)$$

and

$$t_w = f \frac{r V^2}{8}. \quad (9)$$

whrer  $f$  is the friction factor.

The angle,  $\mathbf{q}$ , wetted perimeters,  $Pe$ , interfacial area per unit axial length,  $L_i$ , and the cross-sectional area,  $A$ , can be represented as simple functions of the radius,  $R$ , water level,  $y$ , and/or angle,  $\mathbf{q}$ , as follows:

$$\mathbf{q} = \cos^{-1}\left(\frac{R-y}{R}\right), \quad (10)$$

$$Pe = 2\mathbf{q}R, \quad (11)$$

$$L_i = 2\sqrt{R^2 - (R-y)^2}, \quad (12)$$

and

$$A = R^2\mathbf{q} - \frac{1}{2}L_i(R-y). \quad (13)$$

### 3.2. The model for the RCS water level distribution

As previously indicated, the 90° turn of the fluid at the RV inlet nozzle impacts the level in the operating cold leg. In addition, the phenomenon of hydraulic jump needs to be considered. Hydraulic jump is a local nonuniform flow phenomenon which occurs when the supercritical flow decelerates to subcritical flow. It may be seen from equation (7) that when the Froude number of the fluid approaches unity with a value greater than 1, the differential variation of fluid level in the direction of flow becomes infinity. The result, then, is a marked discontinuity in the surface, characterized by a steep upward slope of the profile. However, it has been a difficult topic to determine the location and the length of the jump even in a rectangular channel (Chow, 1959; White, 1986; Daugherty et al., 1989; Gharangik et al., 1991). Equation (7) must be solved to determine the location and the length of the jump. However, because the geometrical parameters of the cylindrical channel are more complex than those of the rectangular channel, a further study is needed to solve equation (7) and to determine the location and the length of the jump.

In order to model the hydraulic phenomena including the hydraulic jump as well as the effect of 90° turn of the flow direction at the RV inlet nozzle, the operating cold leg is divided into three control volumes as shown in Fig. 3. The second control volume represents hydraulic jump. By noting that the water at the rear side of the SCS injection nozzle is stagnant and all the x-momentum of flow is lost at the downcomer wall, and by assuming the friction loss is negligible, momentum equation (1) for each control volume can then be written as follows:

$$P_0A_0 - P_{1UP}A_{1UP} = \mathbf{r}Q(V_{1UP} - V_{jsur} \cos 60), \quad (14)$$

$$P_{1UP}A_{1UP} - P_{1DN}A_{1DN} = \mathbf{r}Q(V_{1DN} - V_{1UP}), \quad (15)$$

and

$$P_{1DN}A_{1DN} - P_2A_2 = \mathbf{r}Q(-V_{1DN}). \quad (16)$$

where  $V_{jsur}$  is the velocity of the SCS injection flow at the water surface,  $y_{1UP}$ . Considering the gravity acceleration from the top of the SCS injection line,  $y_j$ , to the water surface,  $y_{1UP}$ ,  $V_{jsur}$  will be obtained as,

$$V_{jsur} = \sqrt{V_j^2 + 2g(y_j - y_{1UP})}, \quad (17)$$

where  $V_j$  is the velocity of the SCS injection water at  $y_j$ . Considering the energy loss due to collision with fluid,

the specific energy of the fluid at  $y_{1UP}(x = 0)$  is as follows:

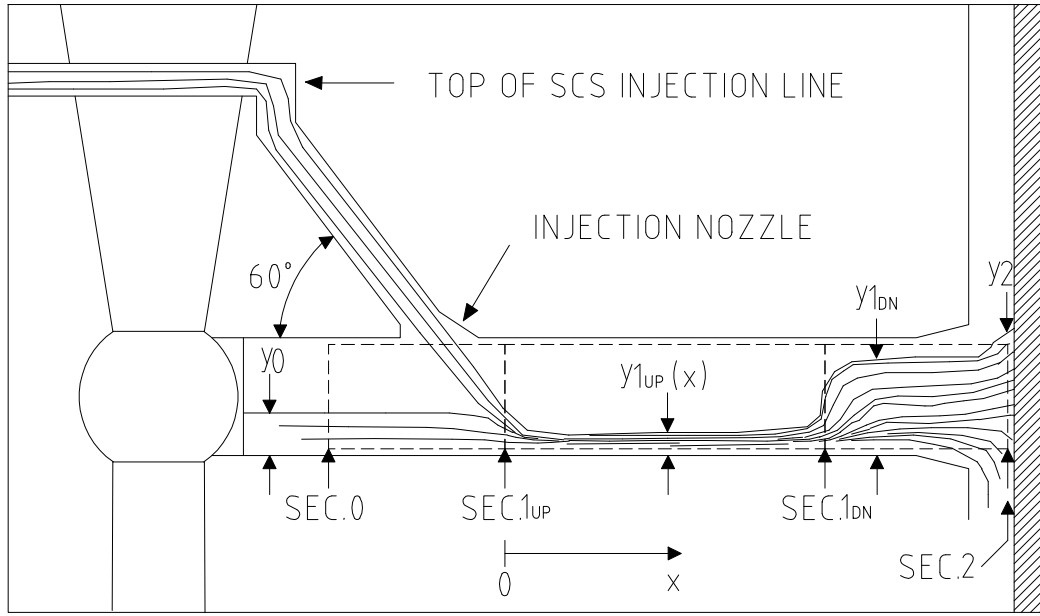


Fig. 3 Three control volumes with hydraulic jump

$$E_{1UP}(x=0) = y_{1UP} + (1 - K_{COL}) \frac{V_{isur}^2}{2g}, \quad (18)$$

where  $K_{COL}$  is the energy loss coefficient and the value of the loss coefficient of a 60° bend is selected.

For a given downstream level,  $y_{1DN}$ , equation (15) results in a quadratic equation with respect to the upstream water level,  $y_{1UP}$ , hence, yields two different values for  $y_{1UP}$ , which correspond to super- and subcritical levels.

The specific energy of the fluid at the jump location is:

$$E_{1UP}(x = L_{jump}) = y_{1UP}(x = L_{jump}) + \frac{V^2(x = L_{jump})}{2g}. \quad (19)$$

$y_{1UP}(x = L_{jump})$  is obtained by solving equation (15) and  $V(x = L_{jump})$  can be obtained from mass continuity equation for a given flowrate. While for a supercritical flow region the excessive energy,  $E_{1UP}(x=0) - E_{1UP}(x = L_{jump})$ , is set equal to the energy dissipated by the wall friction, for the subcritical region the energy dissipation is neglected. This approach is reasonable because the velocity of the subcritical flow is negligibly small compared to that of the supercritical flow. Then, using the Manning formula (Daugherty, 1989), the location of the jump,  $L_{jump}$ , is determined by

$$L_{jump} = \frac{E_{1UP}(x=0) - E_{1UP}(x = L_{jump})}{S}, \quad (20)$$

where

$$S = \left( \frac{nV}{R_h^{2/3}} \right)^2. \quad (21)$$

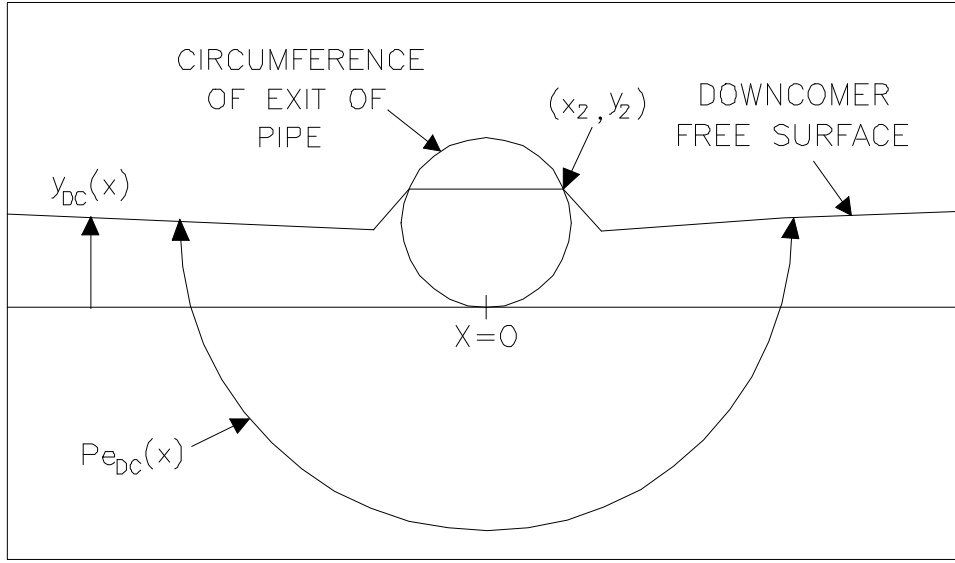


Fig. 4 Water level profile in the operating cold leg and downcomer region

$S$  and  $R_h$  in equation (21) represent the slope of the energy grade line and hydraulic radius of the flow channel, respectively and  $n$  is a constant in the Manning formula. If the supercritical level yields the value of  $L_{jump}$  less than or equal to 0, the level is not physically acceptable, which means that the hydraulic jumps can not occur. Then,  $y_{IUP}(x > 0)$  is set equal to  $y_{IDN}$  and  $y_{IUP}(x = 0)$  is set equal to the stagnant water level,  $y_0$ . As indicated above, the solution for an upstream level,  $y_{IUP}$ , requires the knowledge of a downstream level,  $y_{IDN}$ . In order to determine  $y_{IDN}$  using equation (16), the level at the exit of the cold leg should be known. If we consider  $\overline{y_{DC}}$  as a average water level in the downcomer region, the water level at the exit of the operating cold leg is assumed to be given by

$$y_2 = \overline{y_{DC}} + K_B \frac{Q^2}{d_{DC}^5 i^2}, \quad (22)$$

where  $K_B$  is defined in this analysis as the water level buildup factor and the value of 1.05 is chosen which best fits the overall trend of the RCS water level distribution.

The average water level in the downcomer region should be higher than that in the RV upper plenum, which is almost identical to that in the idle hot leg,  $y_{iHL}$ , to overcome the resistance of the RV.  $\overline{y_{DC}}$  can be obtained by

$$\overline{y_{DC}} = y_{iHL} + K_{DF} \frac{V^2}{2g}, \quad (23)$$

where  $K_{DF}$  is the flow resistance coefficient between the free surface of the downcomer and the RV upper plenum.

To determine the water level in the idle cold leg, the free surface profile of the water in the downcomer region must be known. At any location on the free surface in the downcomer region the following equation holds:

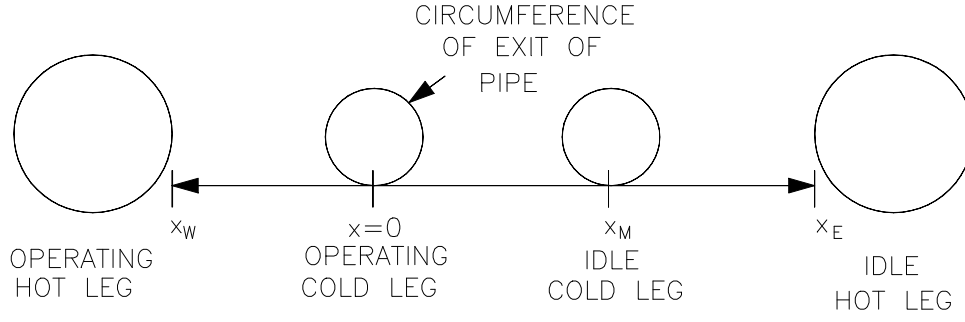


Fig. 5 Half view of flat downcomer region

$$H_{DC} = y_{DC}(x) + \frac{V_{FS}^2(x)}{2g}, \quad (24)$$

where  $V_{FS}(x)$  is the velocity of the fluid at the free surface. In order to determine  $V_{FS}(x)$  accurately a rigorous 3-dimensional analysis needs to be done. However, for calculational simplicity, the velocity of the fluid at the free surface of the downcomer region is assumed to be inversely proportional to the length of the wetted circumference of the circle centered on the axis of the operating cold leg submerged in the water (see Fig. 4), i.e.,

$$V_{FS}(x) = \frac{Q}{A_{DC}(x)}, \quad (25)$$

where  $A_{DC}(x) = d_{DC} Pe_{DC}(x)$ .  $d_{DC}$  is the downcomer gap size and  $Pe_{DC}(x)$  is the perimeter of free surface as shown in Fig. 4. For calculational simplicity Bernoulli constant in equation (24) is assumed to be the same as the average water level in the downcomer region. The level profile based on this model is schematically shown in Fig. 4. Fig. 5 shows half view of symmetrical flat downcomer region.

At the entrance of the RV outlet nozzle (hot leg nozzle), water level drops due to the increase of dynamic head and entrance loss. The water level at the operating hot leg nozzle,  $y_E$ , can be expressed as

$$y_E = y_{iHL} - (1 + K_E) \frac{V_E^2}{2g}, \quad (26)$$

where  $y_E$ ,  $V_E$ , and  $K_E$  are the water level, velocity, and the entrance loss coefficient at the hot leg nozzle, respectively. In order to account for the level drop from the entrance of the hot leg pipe to the SCS suction nozzle, equation (7) is integrated over the flow path, i.e.,

$$y_{oHL} = y_E - \int_0^{L_{HL}} \frac{dy}{dx} dx, \quad (27)$$

where  $L_{HL}$  is the distance between the SCS suction nozzle to the end of the RV outlet nozzle.

It may be seen from the foregoing that if a water level at any component in the RCS is known, all the levels can be determined successively. However, such information is not available. Hence, the solution should start with an assumed level. The appropriateness of the assumed level is checked by using water volume conservation before and after the SCS pump operation. The initial water volume in the RCS can be determined by using the measured initial RWL. If the relative error of the calculated total RCS water volume,  $e_{VOL}$ , defined as

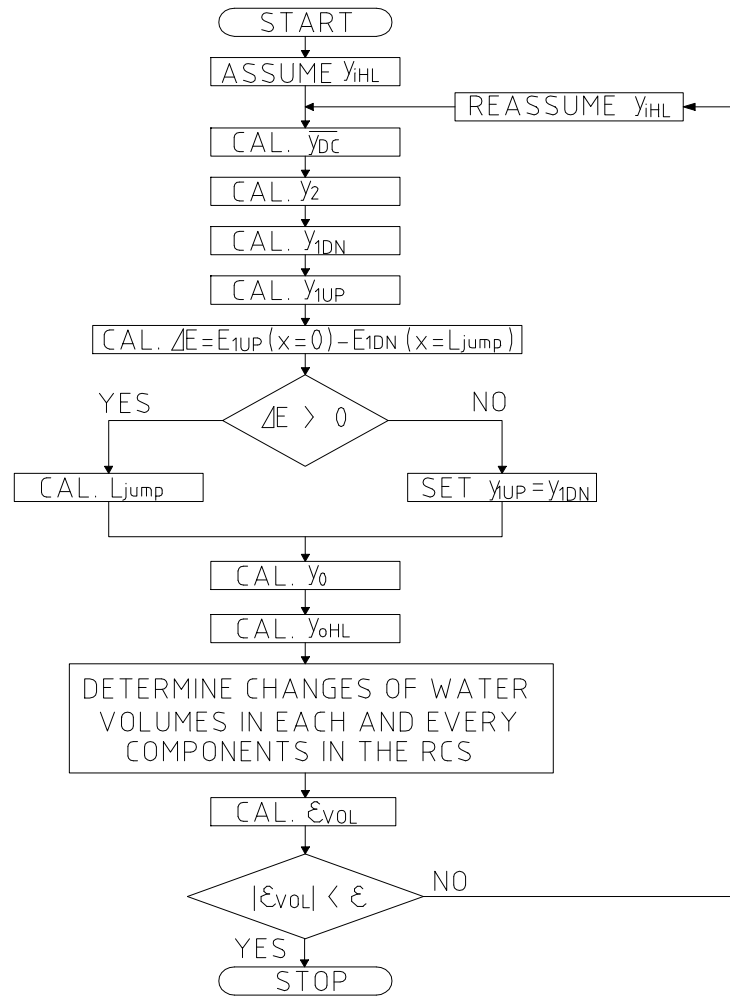


Fig. 6 Solution procedure

$$e_{Vol} \equiv \frac{\text{calculated total water volume} - \text{initial water volume}}{\text{initial water volume}}, \quad (28)$$

falls within the convergence criteria, the assumed level is considered adequate. A brief solution scheme is shown in Fig. 6. A summary of the values of the coefficients and factors used in this analysis is shown in Table 3.

Table 3 Values of various coefficients and factors used in the analysis

Parameter	Description	Value
$K_{DF}$	Resistance coefficient of reactor vessel	15.21
$K_B$	Buildup factor at the exit of operating cold leg	1.05
$K_{COL}$	Collision loss coefficient of SCS Injection flow	0.15
$K_E$	Entrance loss coefficient at operating hot leg nozzle	0.5
$n$	Manning roughness coefficient	0.013
$f$	Friction factor in the wall of operating hot leg	0.0145

Table 4 Summary of calculational results

iRWL cm	Q LPM	$y_0$ cm	$y_{1UP}$ cm	$y_{1DN}$ cm	$y_2$ cm	$y_{iCL}$ cm	$y_{iHL}$ cm	$y_{oHL}$ cm	$E_j$ cm	$E_{jL}$ cm	$E_{1UP}$ cm	$Fr_{1UP}$	$L_{jump}$ cm	$y_{DC}$ cm
7.32	9500	0.2	9.58	9.58	10.5	7.01	7.12	6.36	235	2.28	9.94	0.13	0	7.32
	11500	-0.53	10.8	10.8	12	6.97	7.02	5.9	241	2.97	11.3	0.15	0	7.32
	13000	-1.69	-32.2	12.1	13.5	7.23	7.23	5.8	246	3.59	196	10.7	13.3	7.61
	15000	-1.13	-31.4	14.3	15.9	7.83	7.77	5.87	253	4.57	179	9.63	61.6	8.27
	17000	-0.32	-30.7	16.5	18.4	8.37	8.22	5.8	261	5.73	170	8.94	105	8.86
5.08	9500	-2.52	7.59	7.59	8.58	4.75	4.85	4.01	235	2.24	7.98	0.14	0	5.05
	11500	-3.89	-32.6	9.21	10.5	5.04	5.08	3.86	241	2.93	189	10.9	17.3	5.38
	13000	-3.6	-32	10.8	12.3	5.52	5.52	3.97	246	3.56	172	9.92	57.3	5.89
	15000	-2.92	-31.2	13.1	14.8	6.1	6.03	3.98	253	4.54	159	9.02	106	6.53
	17000	-1.95	-30.5	15.4	17.4	6.58	6.43	3.79	261	5.7	154	8.45	148	7.07
0	9500	-8.73	-33	3.98	5.12	0.48	0.56	-0.46	235	2.16	156	10.5	57.8	0.76
	11500	-8.43	-32.1	6.23	7.65	1.16	1.21	-0.28	241	2.85	135	9.05	121	1.5
	13000	-7.9	-31.5	8.03	9.65	1.6	1.6	-0.28	246	3.47	127	8.39	162	1.98
	15000	-6.83	-30.7	10.6	12.5	2.06	1.99	-0.52	253	4.47	124	7.84	207	2.49
	17000	-5.35	-30.1	13.3	15.4	2.32	2.18	-1.1	261	5.63	126	7.54	239	2.82
-5.08	9500	-13.9	-32.4	0.88	2.2	-3.48	-3.4	-4.67	235	2.07	103	8.39	170	-3.2
	11500	-13.1	-31.5	3.49	5.09	-2.87	-2.83	-4.67	241	2.76	95.6	7.53	233	-2.54
	13000	-12.2	-30.9	5.57	7.37	-2.56	-2.56	-4.92	246	3.39	95.1	7.18	269	-2.18
	15000	-10.3	-30.3	8.57	10.6	-2.42	-2.48	-5.72	253	4.4	99.5	6.96	299	-1.98
	17000	-7.68	-29.8	11.9	14.2	-2.75	-2.87	-7.34	261	5.58	110	6.99	302	-2.23

#### 4. Comparison of the predicted results with measured data

##### 4.1. Test data evaluation

The measured water levels are illustrated on Figures 7 and 8 as functions of the initial RWL and the SCS flowrate. In these Figures, the level data are converted to the relative values with respect to the hot leg center line for convenience. The followings are the facts found in the evaluation of the test data.

- (1) The levels in the operating cold legs are, in general, lower than those in other legs. For a given initial RWL, the level of the operating cold leg decreases as the RCS flow increases up to a certain point and further increase of the flowrate results in the increase of the level. The point where the minimum level occurs tends to move toward lower flowrates as the initial RWL decreases.
- (2) The level in the operating hot leg decreases as the SCS flowrate increases. For a given SCS flowrate, the levels in the operating hot leg are lower than those in the idle legs with the exceptions of several points at higher initial RWL and low SCS flowrates. The level differences increase with the SCS flowrate.
- (3) The levels in the idle loop increase with the increase of the SCS flowrate.
- (4) The scattering of the measured levels, especially the levels between the operating cold legs, is more pronounced at a lower initial RWL and a higher SCS flowrate.
- (5) In the case of the initial RWL of 0.0 cm, the measured levels in loop 2 during loop 1 operation are higher than

those in loop 1 during loop 2 operation.

#### 4.2. Comparison of the predicted results with the test data

Table 4 summarizes the analysis results. In this Table, the calculated level and the specific energy are converted to the relative values with respect to the hot leg center line for convenience. The water levels calculated from the suggested model are compared with the measured data in Figures 7 and 8. In the model, the cold leg level measurement points are symmetric about the axis of hot legs and are treated the same and only one value is given for a given flowrate for a given initial RWL. As can be seen in these figures, the trends, as well as the calculated values, of the RCS water levels are in good agreement with the measured data. From these results the followings are found :

The trends of the RCS water level distribution described above are normally expected except the case of operating cold legs. Considering the driving force, the level in the operating cold leg should be higher than that in the idle hot leg. Therefore, it is concluded that the observed level depression occurs only in the rear side of the SCS injection nozzle and is caused by the drag of the SCS injection flow. However, if the level depression is caused only by the drag, the level of the operating cold leg should decrease monotonically with the SCS flowrate. Hence, other hydrodynamic mechanism which results in a significant level buildup in the downstream of the injection front, thus, replenishing to the water of the rear side is expected to occur. It can be seen, upon summation of equations (14) to (16), that the level in the rear side of the injection front,  $y_0$ , is dependent only on the flowrate of the SCS injection water and the water level at the exit of the operating cold leg,  $y_2$ . It should be noted that the value of  $y_2$  is affected by the downstream levels and that the downstream levels are influenced by the amount of water transferred from the operating loops. The mass transfer from operating loops will eventually influence the level,  $y_0$ . Therefore it would be necessary to consider the hydraulic jump and the level buildup due to the momentum loss at the exit of the operating cold leg. It was found from calculation results that without introducing a hydraulic jump model the parabolic level behavior in the operating cold leg still exists but is less pronounced and the levels in all other legs are monotonically decreasing as the flowrate increases. Based on these, it is concluded that both the hydraulic jump and the level buildup due to the momentum loss at the exit of the operating cold leg are important contributors in determining the water level profile in the operating cold leg. Further, a close review of Table 4 reveals that in most cases the energy of the injection flow is large enough to make the flow in the operating cold leg supercritical and that the hydraulic jump easily occurs at lower initial RWL. The location of the jump increases with the SCS injection flowrate. Thus, sweeping larger amounts of water from the operating cold leg, resulting in higher water levels in the idle loop. This is consistent with what was observed in the test. The foregoing clearly show that the overall behavior of the RCS water levels is strongly attributed to by hydraulic jump.

Although the model suggested in this study incorporates several simplifying assumptions such as energy loss in equation (18), water level buildup model in equation (22), and velocity profile in equation (24), preliminary sensitivity analyses indicate that the use of these assumptions has little impact on the overall trends of the prediction.

The differences in the measured levels between loop 1 and loop 2 operation in the case of initial RWL of 0.0 cm

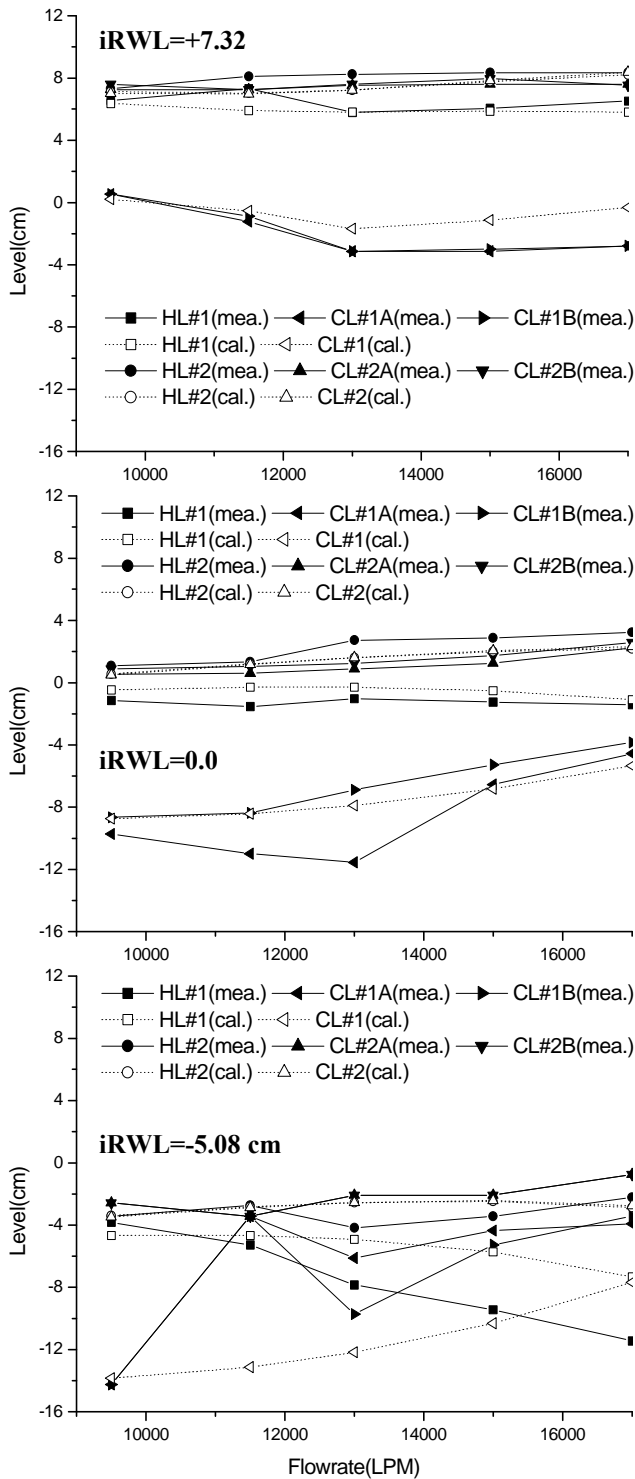


Fig. 7 The comparison of test data and calculated results for loop 1 operation

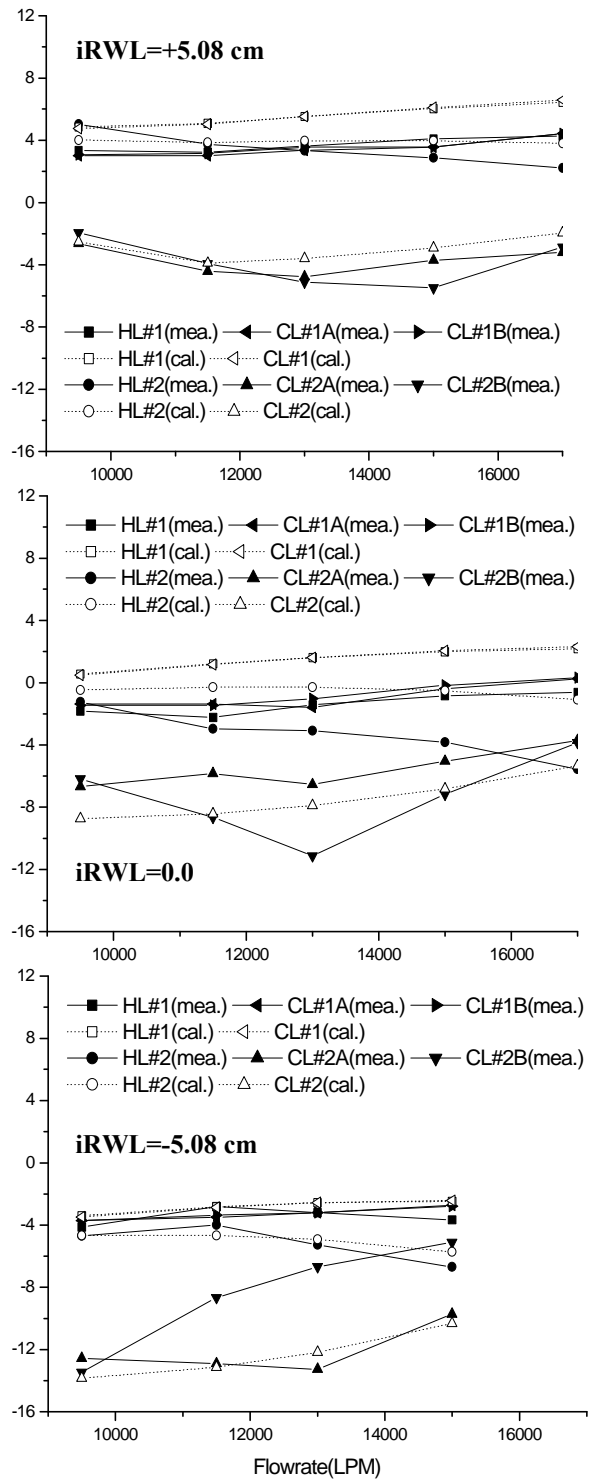


Fig. 8 The comparison of test data and calculated results for loop 2 operation

is not well understood. However, the comparison of the test data with the predicted results indicates that the water volume in the RCS during loop 2 operation is less than that during loop 1 operation. A possible explanation would be the difference in void volume in the SCS injection piping. However, due to the lack of detail information of the SCS during the test, this cannot be confirmed.

The level of the RV inside, which is a parameter directly influenced by the water volume transferred from the operating legs, affects the change in the cross-sectional area of the flow at the entrance region of the hot leg nozzle. Therefore the level profile in the operating hot leg is strongly influenced by the water volume transfer from the operating loop to the RV inside. However, with water level in the idle hot leg lowered below hot leg center line, the water level in the operating hot leg obtained from the test data is lower than that from the calculated result. This is partially due to the phenomenon of the local free fall and swirling at the entrance region of the SCS suction, which is not modeled in this analysis.

## 5. Conclusion

The major factors affecting the RCS water level behavior during mid-loop operation are the SCS return water momentum, water level buildup at the RV inlet nozzle, water level drop at the operating hot leg, and water volume transfer from the operating loop to the RCS. Water volume transfer strongly affects the overall water level behavior. The locations of water volume transfer are the operating hot leg, the stagnant region in the operating cold leg, and the supercritical flow region in the operating cold legs. The volume removal swept by supercritical flow upstream of the operating cold legs is the strongest mechanism of the volume transfer. It is clear that the volume transfer effect in the post-core condition is stronger than that in the pre-core condition because of the reduction of net water volume in the RV. This, in conjunction with the increased flow resistance of the RV, limits the operational band of the mid-loop operation in the post-core condition.

## References

- Andreychek, T. S., et al., 1988. Loss of RHRS cooling while the RCS is partially filled. WCAP-11916, Rev.0, Westinghouse Electric Co.
- Chow, V. T., 1959. Open Channel Hydraulics. McGraw-Hill Book Co., Inc., New York.
- Chung, M. K., et al., 1993. Experiments on Air Entrainment into SCS by Vortex Formation during Mid-Loop Operation. KAERI/TR-357/93, Korea Atomic Energy Research Inst.
- Crutchfield, D. M., 1988. Loss of Decay Heat Removal. USNRC Generic Letter 88-17.
- Daugherty, R. L., Franzini, J.B., and Finnemore, E.J., 1989. Fluid Mechanics with Engineering Application. McGraw-Hill Book Company, Singapore, pp. 340-398.
- Gharangik, A. M., et al., 1991. Numerical simulation of hydraulic jump. Journal of Hydraulic Engineering, Vol. 117, No. 9.
- Newton, R. A., 1988. Westinghouse Owners Group Mid-Loop Operations Concerns. Letter to W. Hodges, NRC, from Chairman of Westinghouse Owners Group, OG-88-24.
- Oh, Y. K., 1991. A Study of Vortex Formation on the Free Surface in a Pipe. Ph.D Dissertation, Kyunghee Univ., Seoul, Korea.
- Sadatomi, M., et al., 1993. Prediction of liquid level distribution in horizontal gas-liquid stratified flows with interfacial level gradient Int. J. Multiphase Flow Vol. 19. No. 6, 987-997.
- USNRC, 1987. Loss of Residual Heat Removal System, Diablo Canyon, Unit 2, April 10, 1987. NUREG-1269.
- White, F. M., 1986. Fluid Mechanics, 2nd ed. 1986. McGraw-Hill Book Company, New York, pp 593-632.